NJC

Accepted Manuscript

This is an *Accepted Manuscript*, which has been through the Royal Society of Chemistry peer review process and has been accepted for publication.

Accepted Manuscripts are published online shortly after acceptance, before technical editing, formatting and proof reading. Using this free service, authors can make their results available to the community, in citable form, before we publish the edited article. We will replace this *Accepted Manuscript* with the edited and formatted *Advance Article* as soon as it is available.

You can find more information about *Accepted Manuscripts* in the Information for Authors.

Please note that technical editing may introduce minor changes to the text and/or graphics, which may alter content. The journal's standard Terms & Conditions and the Ethical guidelines still apply. In no event shall the Royal Society of Chemistry be held responsible for any errors or omissions in this *Accepted Manuscript* or any consequences arising from the use of any information it contains.

ROYAL SOCIETY OF CHEMISTRY

www.rsc.org/njc

Cite this: DOI: 10.1039/c0xx00000x

www.rsc.org/xxxxxx

ARTICLE TYPE

Facile synthesis of Ag nanowires/mesoporous TiO_2 core-shell nanocables with improved properties for lithium storage

GenLong Qu,[a] Hongbo Geng,[a] Jun Guo,[b] Junwei Zheng,[c] Hongwei Gu*[a]

In this paper, mesoporous structured TiO_2 layer coating Ag nanowire coaxial nanocable (denoted as Ag/TiO_2) was successfully fabricated through a facile sol-gel method combined with hydrothermal treatment process and short post-annealing procedure. The composite nanostructures show the unique feature of a uniform core-shell structure with high crystalline nanocrystals, small size (~6 nm), uniform mesoporous (~9 nm), high surface areas (~93.6 m^2 g^{-1}) and highly conductive Ag nanowire favor excellent electrochemical performance of the Ag/TiO_2 nanocables electrode. The resultant Ag/TiO_2 nanocable could deliver superior lithium storage capability (a stable reversible capacity of ~160 mA h g^{-1} after 230 cycles at a current density of 1 C).

Introduction

Lithium ion batteries (LIBs) are of considerable importance in energy storage for portable electronic equipment and electric vehicles due to their high energy and power density, excellent cycling performance and environmental benignity.[1-5] There is no doubt that the anode materials play a decisive role in the performance of LIBs in a large part. In recent years, tremendous efforts have been devoted to the carbon-based anode materials. As a result of the relatively low lithium intercalation voltages, lithium dendrites on the electrode could appear during the charge and discharge process which will cause the safety concern.[6-8] Therefore, developing novel anode materials with suitable voltage platform is still an urgent need. Recently, titanium dioxide (TiO_2) has attracted great attention as promising anode materials for LIBs due to its inherent chemical stability, low cost, transparency and minimal toxicity compared to traditional carbon-based electrode materials.[9, 10] More importantly, the relatively high lithium insertion voltage of TiO_2 electrode materials (>1.5 V vs. Li^+/Li) can not only efficiently alleviate the formation of solid electrolyte interfaces (SEI) layers, but also avoid electroplating of lithium after successful cycles.[11-13] However, the intrinsic poor electronic conductivity and lithium ion diffusivity of TiO_2 electrode materials are detrimental to the cycling performance at high charge and discharge rate, which still remains to be a challenge for TiO_2 as anode materials in practical LIBs application.[14]

To overcome the above problems, several general approaches have been utilized to improve the lithium ion diffusion kinetics and the electronic conductivity, which could lead to largely enhanced cycling and rate performances.[15] Among them, TiO_2-based electrode materials with diverse morphologies (e.g. 3D porous,[16] and hollow spheres,[17] 1D nanotubes,[18] and nanowires,[19] etc.) have drawn special attention because the unique architectures could shorten the diffusion path for electronic, enlarge the electrode/electrolyte interfacial area and ionic transport during the charge and discharge process, allowing the electrode materials to exhibit superior electrochemical performances. Another effective method is to fabricate hybrid nanostructured electrode materials such as the incorporation of TiO_2 with high conductivity materials (e.g. Au,[20] Ni,[21] carbon nanotubes,[22-24] graphene[25-28]), TiO_2-based advanced materials (e.g. $Li_4Ti_5O_{12}$,[29] RuO_2,[30] MoO_2,[31] Fe_2O_3[32, 33]), with excellent cycling stability. Currently, 1D hybrid TiO_2-based materials have been applied as electrode materials giving excellent electrochemical properties. For example, Kim et al. have reported that Ag or Au nanoparticles embedded one-dimensional composite TiO_2 nanofibers can improve Li-ion storage performance through changes in crystallinity and charge transfer upon Ag or Au incorporation.[34] And Yang et al. have demonstrated that the unique orderly-bonded nanostructure, porous characteristics, and highly conductive carbon matrix favour excellent electrochemical performance of the TiO_2@carbon nanofiber electrode.[35] In addition, considerable efforts have been focused on the electrode materials with core-shell structures, which can deliver superior cycling performance and rate properties.[36-38] Therefore, the preparation of core-shell nanostructured titanium dioxide electrode materials is a valid method to improve the performance in LIBs.

Herein, we demonstrate a simple way for synthesis of self-assembled hybrid nanocables composed of Ag nanowires core as conductive phases and mesoporous TiO_2 shell to enhance high rate performance. The resultant Ag/TiO_2 nanocables show a uniform core-shell structure with high crystalline nanocrystals and small

size (~6 nm), uniform mesoporous (~9 nm) and high surface areas (~93.6 m^2 g^{-1}). Most importantly, the Ag/TiO_2 nanocables show a high rate capability and excellent cycle performance (a highly reversible capacity of 160 mA h g^{-1} after 230 cycles at a current density of 1 C) when being used as an anode material for LIBs.

Results and discussion

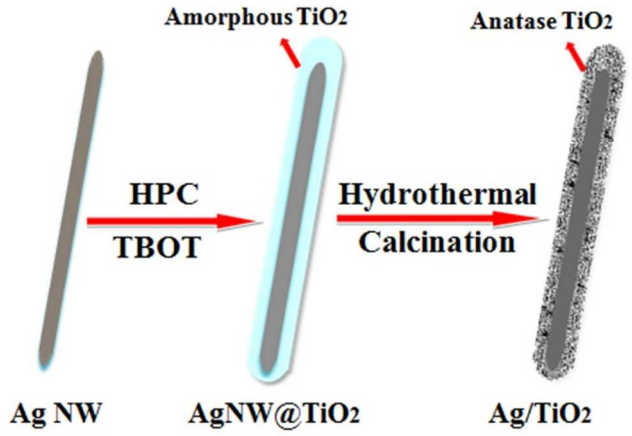

Scheme 1. The synthetic protocol of the Ag/TiO_2 nanocable.

As shown in Scheme 1, the Ag/TiO_2 nanocables were prepared by a facile route. Firstly, Ag nanowires and hydroxypropyl cellulose (HPC) were dispersed in absolute ethanol by ultra-sonication, followed by adding tetrabutyl titanate (TBOT) as the Ti precursor. During the sol–gel process, amorphous TiO_2 layer was uniformly deposited on the Ag nanowire by the hydrolysis of TBOT (AgNW@a-TiO_2 nanocables). The amorphous TiO_2 layer was treated via hydrothermal treatment to form mesoporous TiO_2 layer (AgNW@m-TiO_2 nanocables). Subsequently, the samples were annealed at 500 °C under an argon atmosphere to obtain the final mesoporous hybrid composites (Ag/TiO_2 nanocables). As the anode materials for LIBs, the Ag/TiO_2 nanocables showed a high lithium storage capacity (an initial discharge capacity of 181 mA h g^{-1} at a current density of 168 mA g^{-1}), long cycling performance (a perfect reversible capacity of ~160 mA h g^{-1} after 230 cycles at a current density of 168 mA g^{-1}). The Ag/TiO_2 nanocables were found to be effective for energy storage which enhanced the electrical conductivity and facilitated the penetration of the electrolyte.

In Figure 1, the morphologies of the as-prepared AgNW@a-TiO_2 and AgNW@m-TiO_2 nanocables were characterized by scanning electron microscope (SEM) and transmission electron microscope (TEM), respectively. Figure 1a shows the SEM image of the as-prepared AgNW@a-TiO_2 nanocables, which clearly indicate that the uniform TiO_2 layers have been well coated on the surface of Ag nanowires. The original surface of the Ag nanowires is quite smooth, as demonstrated in Figure S1. In addition, the TEM image (Figure 1c) describes that the average thickness of amorphous TiO_2 shell was about 40 nm. Then, the AgNW@m-TiO_2 nanocables were formed through hydrothermal treatment, which were analyzed by SEM and TEM. Both the SEM image (Figure 1b) and TEM image (Figure 1d) reveal that the sample is composed by mesoporous TiO_2 layer and intact silver nanowires core, suggesting that the structure of AgNW@m-TiO_2 nanocables are quite stable. It is clearly found that the AgNW@m-TiO_2 nanocables exhibit a rough surface made up of continuous TiO_2 nanoparticles.

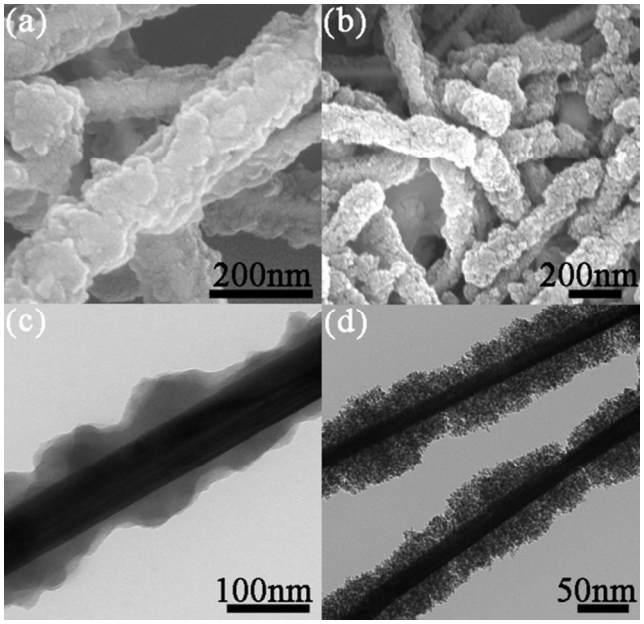

Figure 1. (a) SEM and (c) TEM images of AgNW@a-TiO_2 nanocables; (b) SEM and (d) TEM images of the AgNW@m-TiO_2 nanocables.

The detailed structures of as-obtained Ag/TiO_2 nanocables were further observed by TEM imaging (Figure 2c–e). From the magnified TEM image of one corner of a single Ag/TiO_2 nanocable (Figure 2d), it can be observed that the shell is constructed by nanoparticles with size of about 6 nm. Moreover, high-resolution TEM (HRTEM) analysis was also carried out (Figure 2e): the width of 0.35 nm between neighboring lattice fringes were clearly observed, suggesting that the highly crystalline nature of the TiO_2 nanoparticles, in good agreement with the (101) lattice spacing of anatase TiO_2. The selective area electron diffraction (SAED) pattern of TiO_2 shell shown in Figure 2f indicates a diffuse ring, which implies the existence of polycrystalline properties.

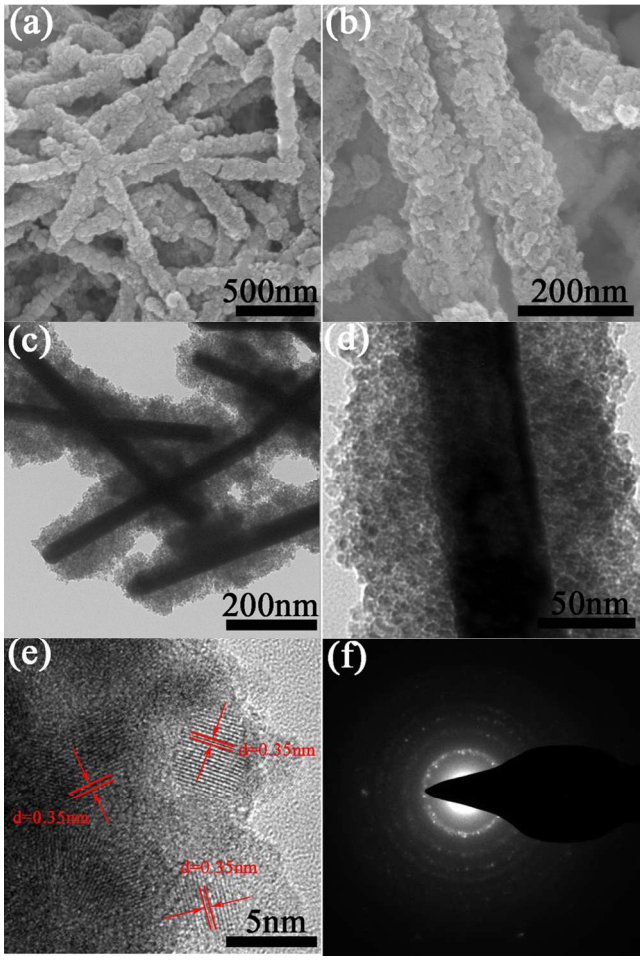

Figure 2. SEM (a, b), TEM (c, d) and HRTEM (e) images of the Ag/TiO_2 nanocables, (f) the SAED pattern of the Ag/TiO_2 nanocables.

The crystallographic structure of the as-prepared Ag/TiO_2 nanocables was investigated by X-ray diffraction (XRD). And the XRD pattern of the Ag/TiO_2 nanocables is illustrated in Figure 3a. Obviously, no additional peaks arise in the XRD pattern, indicating that no impurities were present. All the diffraction patterns are well indexed to the anatase phase (JCPDS card no. 21-1272). Additionally, diffraction peaks of Ag were also found in the patterns of the Ag/TiO_2 nanocables, indicating that the Ag nanowire composite dispersed in TiO_2 nanoparticles. Such a unique mesoporous TiO_2 structure with (101) orientated nanoparticles should provide facile interfacial contact with electrolyte and promoted transport kinetics of Li^+ ions.[39]

To further study the chemical composition of the as-prepared Ag/TiO_2 nanocables, the sample was analyzed by X-ray photoelectron spectroscopy (XPS), as shown in Figure 3b-d. The sharp signals in the XPS survey spectrum (Figure S2) are clearly corresponding to the characteristic peaks of Ag 3d, Ti 2p and O 1s, respectively, indicating the existence of silver, titanium, oxygen elements in the sample. Figure 3b exhibits two peaks at 368.1 and 374.2 eV with a spin–orbit splitting of 6.1 eV is strictly verifying the formation of metallic Ag 3d states.[40] Figure 3c displays the Ti 2p spectrum at 464.5 and 459 eV corresponding to Ti 2p1/2 and Ti 2p3/2, respectively, which are characteristic peaks of Ti^{4+}.[41] The O 1s peak at about 530.4 eV (Figure 3d), which belongs to the Ti–O–Ti bonds in TiO_2. The weak peak at about 532 eV may be ascribed to surface –OH or adsorbed water.[42]

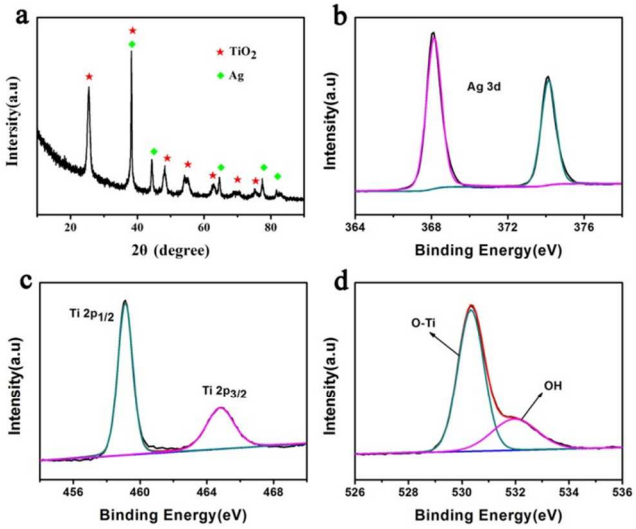

Figure 3. (a) XRD pattern of the Ag/TiO_2 nanocables; (b) Ag 3d, (c) Ti 2p and (d) O 1s XPS spectra of the Ag/TiO_2 nanocables.

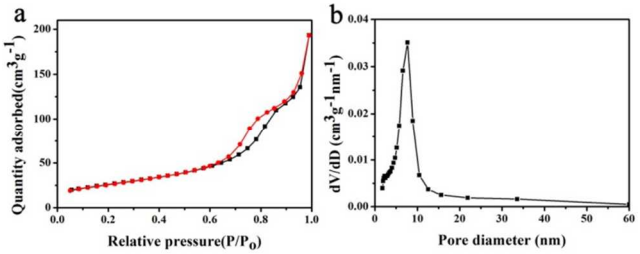

Figure 4. Nitrogen adsorption-desorption isotherms (a), and the pore size distribution curves (d) of the Ag/TiO_2 nanocables.

The mesostructure was measured by nitrogen isothermal absorption–desorption measurements. As shown as Figure 4a, the isotherm curves of Ag/TiO_2 composites show the typical adsorption hysteresis pertaining to type IV isotherm curves, which proves the presence of mesoporous structure.[43] The Brunauer-Emmett-Teller (BET) surface area is 93.6 m^2 g^{-1}, which may be mainly resulted from an aggregation of anatase TiO_2 grains. The sample is regarded as a mesoporous structure with the primary pore size of about 9 nm, which is in accordance with TEM images (Figure 2c and d). These pores are likely to provide the space and path of lithium ion transport. Thereby, the high surface area and mesoporous architectures would be effective factors to improve the electrochemical performance of Ag/TiO_2 nanocables in LIBs.

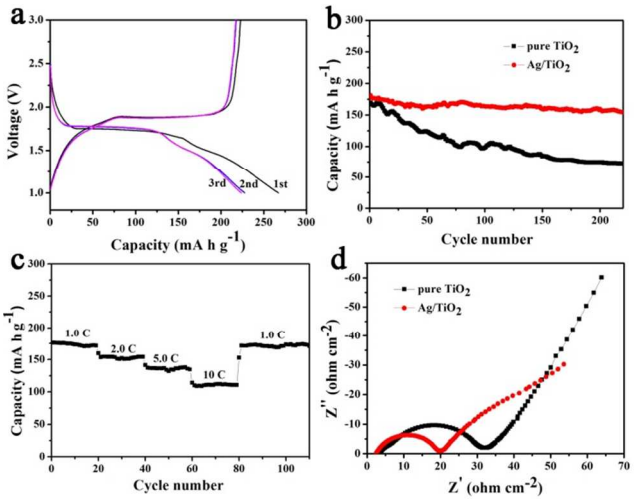

Figure 5. (a) Charge/discharge curves of the Ag/TiO_2 electrode at a current density of 0.1 C; (b) Cycle performance of the pure TiO_2 and Ag/TiO_2 nanocables at a current density of 1 C; (c) Specific capacity of the Ag/TiO_2 nanocables at different current density; (d) Electrochemical impedance spectroscopy (EIS) of TiO_2 and Ag/TiO_2 as the working electrode before cycling.

We explored the application of Ag/TiO_2 nanocables composites as the anode material in lithium ion batteries. Figure 5a shows the typical discharge-charge voltage profiles of the as-prepared samples at a current density of 0.1 C(1 C=168 mA g^{-1}) with a cut-off voltage ranging from 1.0 to 3.0 V versus Li^+/Li, providing two distinct voltage plateaus. The two obvious voltage plateaus in the discharge–charge curves center at approximately 1.7 V and 1.9 V versus Li^+/Li, respectively, which correspond to the lithium insertion/extraction process between anatase TiO_2 and orthorhombic $Li_{0.5}TiO_2$.[44]. The initial discharge and charge capacities of the Ag/TiO_2 nanocables are 267.2 mA h g^{-1} and 222.9 mA h g^{-1}, respectively, indicating a high coulombic efficiency of 83.5%. Figure 5b shows the cycling performance of the pure TiO_2 and Ag/TiO_2 nanocables at a current density of 1 C for 230 cycles in the voltage range of 1.0 to 3.0 V. Compared with the pure TiO_2 electrode, the Ag/TiO_2 nanocables could deliver a larger discharge specific capacity of about 160 mA h g^{-1} after 230 cycles, which was much higher than that of the pure TiO_2 electrode. The excellent performance may be derived from the unique textural specialties such as mesoporous TiO_2 layers, relatively high surface area and conductive Ag NWs, which can effectively facilitate the electron transfer and increased interfacial surface areas for lithium storage. Figure S4 shows the electrochemical performance of the Ag/TiO_2, Ag/TiO_2-0.4 and Ag/TiO_2-0.1 electrodes at the current rate of 0.5 C. Notably, the Ag/TiO_2 electrode exhibits superior cycling performance, which is much higher than that of the Ag/TiO_2-0.4 and Ag/TiO_2-0.1 electrodes. Beyond that, the rate capability of the Ag/TiO2 nanocables are also evaluated at discharge–charge current rates ranging from 1 to 10 C (1 C=168 mA g^{-1}), as shown in Figure 5c. Clearly, it exhibits excellent cyclic capacity with specific capacities of 178.4, 153.8, 138.1 and 111.5 mA h g^{-1} at current rates of 1, 2, 5, and 10 C, respectively. Importantly, after the high-rate discharge–charge cycling, the capacity of the Ag/TiO_2 nanocables can still recover to the initial value when the current density decreases to 1 C, which showed relatively high reversibility.

Furthermore, the electrochemical impedance spectroscopy (EIS) measurements were carried out on both pure TiO_2 and Ag/TiO_2 sample. Figure 5d shows the Nyquist plots recorded for the TiO_2 and the Ag/TiO_2, respectively, which typically consists of a middle-frequency semicircle and a low-frequency inclined line. The middle frequency semicircle correspond to the charge-transfer impedance in the electrode/electrolyte interface.[45] Compared with pure TiO_2, the Ag/TiO_2 composites possessed a smaller R_{ct} value, indicating that the synergistic effect of Ag nanowire and mesoporous structured TiO_2 can effectively improve the electron transport, and can lead to higher discharge/charge capacity. To further investigate the structure change of Ag/TiO_2 core-shell nanocables, the TEM images were examined after 50 cycles at a rate of 1 C. As shown in Figure S5, their original textural properties in terms of shape, size and structural integrity were well maintained, which demonstrates that a high structural stability of the composite 1D core–shell nanocables can be kept under many discharge/charge cycles. The stable cycle performance might be associated with the maintained structural integrity.

The above results clearly demonstrate that the Ag/TiO_2 nanocables exhibit increased lithium storage capacity and remarkable cycling performance in LIBs due to their unique structural characteristics. Firstly, the high surface area of the Ag/TiO_2 nanocables can provide more electrolyte-electrode contact area for Li^+ insertion and significantly enhance surface lithium storage. Secondly, the small size of primary TiO_2 nanocrystallines and the presence of permeable mesoporous shells can effectively enhance the transport of electrolytes and Li^+ on the interface of electrodes, leading to good rate capability.[46] Meanwhile, the mesoporous structure can accommodate large extra space the uniform distribution of the induced stress, which will be beneficial to maintain the structural stability. Thirdly, the Ag NWs work as a conductive medium between TiO_2 nanocrystals and current collector, as well as maintains the stability of the electrode, which contribute to the much improved reversible capacity. All of these features would effectively promote the cycling performance and result in excellent lithium storage properties. As anticipated in Figure S3, The present method is facile and general for synthesis of Ag/SiO_2 and Ag/SnO_2 coaxial nanocables.

Conclusions

In summary, the Ag/TiO_2 nanocables with high purity can be successfully obtained by a facile method. The as-prepared Ag/TiO_2 nanocables consist of a uniform and highly crystalline anatase TiO_2 shell and Ag nanowires core with a high surface area and uniform mesoporous. Such a special and unique architecture of the Ag/TiO_2 nanocables could provide more lithium-storage sites to enhance transport kinetics for both electrons and lithium ions. As a result, the Ag/TiO_2 nanocables deliver a high lithium storage capacity (a perfect reversible capacity of ~160 mA h g^{-1} after 230 cycles at a current density of 1 C). In view of the facile synthesis and excellent electrochemical performance obtained, there nanocables could be a potential candidate as the anode materials for the development of the next generation of high-performance LIBs.

Experimental

All reagents are of analytical purity and used without further purification.

Synthesis of Ag NWs: Silver nanowires were prepared by a previously reported. Typically, 5.86 g PVP (Mw: 55 000, Aldrich) and 190 mL glycerol were added into a 500 mL round bottle flask with tender stirring and heating added until all PVP was dissolved. After cooling to room temperature, 1.58 g silver nitrate powder was added into the solution. Subsequently, a good mixed 10 mL glycerol solution containing 59 mg NaCl and 0.5 mL H_2O was added into the flask. The flask was then heating from room temperature to 210 ^{o}C in 20 minutes and gentle stirring equipped with a PTFE paddle stirrer. When the temperature reached 210 ^{o}C, the heating was stopped and after temperature drops back to room temperature, the products were purified by centrifugation to remove PVP with absolute ethanol several times. The products were collected and dispersed into an absolute ethanol solution for further experiments.

Synthesis of Ag/TiO_2 nanocables: Firstly, 0.2g Ag NWs and 0.1g hydroxypropyl cellulose (HPC) were dispersed in 20ml absolute ethanol by ultra-sonication, followed by addition of 0.1ml deionized water. Subsequently, a good mixed solution containing 3 ml tetrabutyl titanate (TBOT) and 3 ml absolute ethanol were dropwise added to the above solution (0.5 ml / min), after completion of the addition stirring for 100 min at 85 ^{o}C. The resulting solid was dissolved in 40 ml ethanol and 20 ml deionized water, and hydrothermally treated at 160 ^{o}C for 4 h, after being washed with distilled water and ethanol. The impregnated powder was dried in a vacuum oven at 100 ^{o}C overnight, and then calcined in a muffle oven at 500 ^{o}C for 2 h under an argon atmosphere to obtain the mesostructure. Meanwhile, the Ag/TiO_2-0.1 and Ag/TiO_2-0.4 were prepared by varying the amount of Ag NWs to 0.1 g and 0.4 g with keeping other experimental conditions unchanged. The morphologies of the as-prepared Ag/TiO_2-0.1 and Ag/TiO_2-0.4 nanocables were characterized by transmission electron microscope (Figure S3). Through these comparisons we can form this structure with 0.2g Ag NWs very well. The present method is facile and general for synthesis of Ag/SiO_2 and Ag/SnO_2 coaxial nanocables (figure S6).

Materials characterization: The microscopic features of the Ag/TiO_2 nanocables were examined by scanning electron microscopy (SEM), transmission electron microscopy (TEM) and high-resolution TEM (HRTEM). SEM spectroscopy was performed on a Hitachi S-4700 cold field emission scanning electron microscope operated at 30 KV, TEM (TecnaiG220, FEI, American) was obtained by a Gatan CCD794 camera operated at 200 KV and HRTEM was recorded on a Tecani G2 F20 S-TWIN microscope with an accelerating voltage of 200 KV. The crystalline structure was characterized by X-ray diffraction (XRD) using an X'Pert-Pro diffractometer (Netherlands PANalytical) with a Cu Kα X-ray source (λ = 1.540598 Å). The chemical species of the products was analyzed by X-ray photoelectron spectroscopy (XPS, Escalab250Xi, UK) with a hemispherical electron energy analyzer using a monochromatic A1Kα X-ray radiation as the excitation source. High-resolution spectra of the Ag 3d, Ti 2p and O 1s core lines were collected using a pass energy of 20 eV, a step size of 0.05 eV, and a sweep time of 180 s. The nitrogen adsorption-desorption were tested to characterize the micropores of the samples at 77 K using an Autosorb-1 system (Quanta Chrome). The pore size distribution was calculated using the Barrett–Joyner–Halenda (BJH) method based on the adsorption branch.

Electrochemical measurement: The electrochemical measurements of the products were measured using a coin-type half cell (CR 2016). The working electrode was prepared by mixing active material (Ag/TiO_2 nanocables or pure TiO_2), conductive materials (acetylene black, AB), and polymer binder (polyvinylidene difluoride, PVDF) at weight ratio of 80:10:10, dissolving into the N-methyl-2-pyrrolidone (NMP) to form homogeneous slurry, followed by spreading onto a copper foil. And then, the copper foil was dried in vacuum at 110 ^{o}C overnight. The electrolyte was 1 M $LiPF_6$ dissolved in a mixed solution of ethylene carbonate (EC) and diethyl carbonate (DEC) in the weight ratio of 1:1 (Provided by Guotaihuarong, Zhangjiagang, China). Cell assembly was performed in an argon-filled glovebox with the presence percent of moisture and oxygen below 0.1 ppm. The cells were charged and discharged between 3.0 V and 1.0 V at room temperature. The electrochemical impedance spectroscopy (EIS) was carried out by using a CS350 electrochemical workstation at 25 ^{o}C with the frequency range from 100 kHz to 0.01 Hz and an AC signal of 5 mV in amplitude as the perturbation. The specific capacity

was calculated according to the corresponding total weight of active materials in each electrode.

Acknowledgements

This research was supported by the National Natural Science Foundation of China (No. 21373006), and the Priority Academic Program Development of Jiangsu Higher Education Institutions.

Notes and references

[a]*Key Laboratory of Organic Synthesis of Jiangsu Province, College of Chemistry, Chemical Engineering and Materials Science & Collaborative Innovation Center of Suzhou Nano Science and Technology, Soochow University, Suzhou, 215123, China.*

[b]*Analysis and Testing Center, Soochow University,*

[c]*College of Physics, Optoelectronics and Energy, Soochow University, Suzhou, 215006, China*

E-mail: hongwei@suda.edu.cn

† Electronic Supplementary Information (ESI) available: Additional SEM , TEM and XPS.

1 Y. K. Sun, S. T. Myung, B. C. Park, J. Prakash, I. Belharouak, K. Amine, *Nat. Mater.*, 2009, 8, 320.

2 P. G. Bruce, B. Scrosati, J. M. Tarascon, *Angew. Chem. Int. Ed.*, 2008, 47, 2930.

3 H. W. Lee, P. Muralidharan, R. Ruffo, C. M. Mari, Y. Cui, D. K. Kim, *Nano Lett.*, 2010, 10, 3852.

4 P. Lian, X. Zhu, H. Xiang, Z. Li, W. Yang, H. Wang, *Electrochimca. Acta*, 2010, 56, 834.

5 N. Liu, H. Wu, M. T. McDowell, Y. Yao, C. M. Wang, Y. Cui, *Nano Lett.*, 2012, 12, 3315.

6 N. Liu, H. Wu, M. T. McDowell, Y. Yao, C. M. Wang, Y. Cui, *Nano Lett.*, 2012, 12, 3315.

7 S. S. Zhang, K. Xu, T. R. Jow, *J. Power Sources*, 2006, 160,1349.

8 H. K. Kim, S. M. Bak, K. B. Kim, *Electrochem. Commun.*, 2010, 12, 1768.

9 Z. Yang, D. Choi, S. Kerisit, K. M. Rosso, D. Wang, J. Zhang, G. Graff, J. Liu, *J. Power Sources*, 2009, 192, 588.

10 Y. S. Hu, L. Kienle, Y. G. Guo, J. Maier, *Adv. Mater.*, 2006, 18,1421.

11 L. F. Shen, X. G. Zhang, H. S. Li, C. Z. Yuan, G. Z. Cao, *J. Phys. Chem. Lett.*, 2011, 2, 3096.

12 G. N. Zhu, Y. G. Wang, Y. Y. Xia, *Energy Environ. Sci.*, 2012, 5, 6652.

13 H. Kim, M. G. Kim, J. Cho, Adv. Energy Mater., 2012, 2, 1425.

14 H. G. Jung, S. W. Oh, J. Ce, N. Jayaprakash, Y. K. Sun, *Electrochem. Commun.*, 2009, 11, 756.

15 H. Ren, R. B. Yu, J. Y. Wang, Q. Jin, M. Yang, D. Mao, D. Kisailus, H. J. Zhao, D. Wang, *Nano Lett.*, 2014, 14, 6679.

16 H. E. Wang, H. Cheng, C. P. Liu, X. Chen, Q. L. Jiang, Z. G. Lu, Y. Y. Li, C. Y. Chung, W. Y. Zhang, J. A. Zapien, L. Martinu and I. Bello, *J. Power Sources*, 2011, 196, 6394.

17 X. Zhang, V. Aravindan, P. Suresh Kumar, H. Liu, J. Sundaramurthy, S. Ramakrishna, S. Madhavi, *Nanoscale*, 2013,5, 5973.

18 Q. L. Wu, J. C. Li, R. D. Deshpande, N. Subramanian, S. E. Rankin, F. Q Yang, Y. T. Cheng, *J. Phys. Chem. C*, 2012, 116, 18669.

19 Y. Wang, M. Wu, W. F. Zhang, *Electrochim. Acta*. 2008, 53, 7863.

20 B. Hao, Y. Yan, X. B. Wang, G. Chen, *Nanoscale*, 2013, 5, 10472 .

21 W. Wang, M. Tian, A. Abdulagatov, Steven. M. George, Y. C. Lee, R.G. Yang. *Nano Lett.*, 2012, 12, 655.

22 J. Shu, H. Li, R. Z. Yang, Y. Shi, X. J. Huang, *Electrochem. Commun.*, 2006, 8, 51.

23 B. J. Landi, M. J. Ganter, C. D. Cress, R. A. DiLeo, R. P. Raffaelle, *Energy Environ. Sci.*, 2009, 2, 638.

24 H. X. Zhang, C. Feng, Y. C. Zhai, K. L. Jiang, Q. Q. Li, S. S. Fan, *Adv. Mater.*, 2009, 12, 2099.

25 W. Li, F. Wang, S. S. Feng, J. X. Wang, Z. K. Sun, B. Li, Y. H. Li, J. P. Yang, A. A. Elzatahry, Y. Y. Xia, D. Y. Zhao, *J. Am. Chem. Soc.*, 2013, 135, 18300.

26 X. Xin, X. F. Zhou, J. H. Wu, X. Y. Yao, Z. P. Liu, *ACS Nano.*, 2012, 6, 11035.

27 N. Li, G. Liu, C. Zhen, F. Li, L. Zhang, H. M. Cheng, *Adv. Funct. Mater.*, 2011, 21, 1717.

28 S. B. Yang, X. L. Feng, K. Mullen, *Adv. Mater.*, 2011, 23, 3575.

29 T. F. Yi, Z. K. Fang, Y. Xie, Y. R. Zhu, S. Y. Yang, *ACS Appl. Mater. Interfaces*, 2014, 6, 20205.

30 M. J. Armstrong, D. M. Burke, T. Gabriel, C. O'Regan, C. O'Dwyer, N. Petkov, J. D. Holmes, *J. Mater. Chem. A*, 2013, 1, 12568.

31 J. Y. Liao, D. Higgins, G. Lui, V. Chabot, X. C. Xiao, Z. W. Chen, *Nano Lett*, 2013, 13, 5467.

32 X. Zhang, H. X. Chen, Y. P. Xie, J. X. Guo, *J. Mater. Chem. A*, 2014, 2, 3912.

33 W. Li, J. P. Yang, Z. X. Wu, J. X. Wang, B. Li, S. S. Feng, Y. H. Deng, F. Zhang, D. Y. Zhao, J. Am. Chem. Soc. 2012, 134, 11864.

34 S. H. Nam, H.-S. Shim, Y.-S. Kim, M. A. Dar, J. G. Kim, W. B. Kim, *ACS Appl. Mater. Interfaces*, 2010, 2, 2051.

35 Z. X. Yang, G. D. Du, Q. Meng, Z. P. Guo, X. B. Yu, Z. X. Chen, T. L. Guo, R. Zeng, *J. Mater. Chem.*, 2012, 22, 5848.

36 X. Y. Xue, Z. H. Chen, L. L. Xing, S. Yuan, Y. J. Chen, *Chem. Commun.*, 2011, 47, 5205.

37 Q. Wang, D. A. Zhang, Q. Wang, J. Sun, L. L. Xing, X. Y. Xue, *Electrochimica. Acta* , 2014, 146, 411.

38 Q. Wang, J. Sun, Q. Wang, D. A. Zhang, L. L. Xing, X. Y. Xue, *J. Mater. Chem. A*, 2015, 3, 5083.

39 Y. Ren, L. J. Hardwick, P. G. Bruce, *Angew. Chem., Int. Ed.*, 2010, 122, 2624.

40 Q. Xiang, J. Yu, B. Cheng , H. Ong, *Chem. Asian J.*, 2010, 5,1466.

41 Y. Luo, J. Luo, W. Zhou, X. Qi, H. Zhang, Y. Denis, C. M. Li, H. J. Fan and T. Yu, *J. Mater. Chem. A*, 2013, 1, 273.

42 Y. Qiao, X. L. Hu, Y. Liu, C. J. Chen, H. H. Xu, D. F. Hou, P. Hu, Y. H. Huang, *J. Mater. Chem. A*, 2013, 1, 10375.

43 L. F. He, R. G. Ma, N. Du, J. G. Ren, T. L. Wong, Y. Y. Li, S. T. Lee, *J. Mater. Chem A*., 2012, 22, 19066.

44 G. Q. Zhang, H. B. Wu, T. Song, U. Paik, X. W. Lou, *Angew. Chem. Int. Ed.*, 2014, 53, 12590.

45 L. W. Su, Z. Zhou, M. M. Ren, *Chem. Commun.* 2010, 46, 2591.

46 M. Wagemaker, W. J. H. Borghols, F. M. Mulder, *J. Am. Chem. Soc.*, 2007, 129, 4323.